

MONITORING THE SPACE DEBRIS ENVIRONMENT AT HIGH ALTITUDES USING DATA FROM THE ESA OPTICAL SURVEYS

T. Schildknecht

Astronomical Institute, University of Bern, CH-3012 Bern, Switzerland
thomas.schildknecht@aiub.unibe.ch

**R. Musci¹, T. Flohrer¹,
W. Flury², J. Kuusela³,
J. de Leon⁴, L. de Fatima Dominguez Palmero⁴**

¹Astronomical Institute, University of Bern, CH-3012 Bern, Switzerland

²ESA ESOC, Robert-Bosch-Strasse 5, 64293 Darmstadt, Germany

³ASRO, Turku, Finland

⁴Instituto de Astrofísica de Canarias, 38200 La Laguna, Tenerife, España

ABSTRACT

In the framework of its space debris research activities ESA established an optical survey program to study the space debris environment at high altitudes, in particular in the geostationary ring and in the geostationary transfer orbit region. The Astronomical Institute of the University of Bern (AIUB) performs these surveys on behalf of ESA using ESA's 1-meter Telescope in Tenerife. Regular observations were started in 1999 and are continued during about 100 nights per year. Results from these surveys revealed a substantial amount of space debris at high altitudes in the size range from 0.1 to 1 meter. The data was also used as input to generate ESA's MASTER population model and to validate further tools like PROOF.

Several space debris populations with different dynamical properties were identified in the geostationary ring. There is in particular a series of clusters in the orbital element space. Members of these clusters have very similar orbital planes. This in turn led to the hypothesis that the clusters were generated by explosive events, either real explosion or collisions. The data shows at least 8 distinct clusters whereas only two explosions are known to have occurred in the geostationary ring (a breakup of an Ekran spacecraft in 1978 and an explosion of a Titan rocket upper stage in 1992). The consistent ESA data set from the optical surveys offers the unique possibility to monitor these clusters, and the high-altitude debris environment in general over a time span of more than 5 years. The observed evolution of the clusters will be compared with the results from simulations, where the orbits of the observed clusters are propagated using numerical integration.

INTRODUCTION

In the framework of its space debris research activities ESA established a long-term optical survey program to study the space debris environment at high altitudes. For this purpose the ESA 1-meter telescope at Tenerife, Canary Islands, was equipped with dedicated focal reducer optics and a 4k x 4k CCD mosaic CCD camera. First space debris observations with this instrument were obtained in 1999. Continuous surveys were started in 2001. Since then the telescope is scheduled for space debris observation during about 120 to 140 nights per year. The observations are performed in two-week intervals centered on New Moon. In the average about 75% of the scheduled nights turned out to be of good quality, i.e. cloudless for more than four hours. An overview of the ESA surveys is given in Table 1.

The early surveys focused on the detection of debris in the geostationary ring (GEO). Since mid of 2002 part of the observation time is devoted to searches for objects in elliptical orbits. The latter were optimized to find debris in geostationary transfer orbits (GTO), in particular in the region occupied by Ariane upper stages.

An increasing fraction of the telescope time is used for so-called follow-up observations, i.e. to re-observe objects in order to determine their orbits. Additional follow-up measurements are performed with the 1-meter telescope of the Astronomical Institute of the University of Bern, located in Zimmerwald, Switzerland.

RESULTS FROM THE CONTINUOUS SURVEYS

The technique to detect space debris at the ESA telescope is based on the comparison of frames of the same stellar field taken at different epochs. Objects in GEO or GTO cross the 0.7° field of view of the ESA space debris camera in a few minutes when the telescope is essentially tracking the stars. On average such an object is detected on two to three frames. Given a rate of one frame per minute a ‘detection’ of an objects consists of a short track of two to three observations spanning an interval of two to three minutes. (There are actually frames taken every 30 seconds but as we observe two stellar fields ‘in parallel’ only each second frame pertains to the same field.) Each of these tracks thus provides a small series of astrometric positions, as well as apparent magnitudes. A single track covers only a very small part of the orbit, usually a few 10^{-3} of a

full revolution. Observations from a single track therefore do not allow determining a full 6-parameter orbit, but only circular orbits. The latter approximation is reasonable for objects in or near the GEO region but is obviously completely inappropriate for objects in GTO or other highly elliptical orbits. In order to acquire at least some statistical information on the orbits, follow-up observations of a subset of the detected objects are performed and – if successful – 6-parameter orbits are derived.

Each detection is correlated with the ESA DISCOS catalogue of orbital elements. The correlation process is based on comparing the positions, apparent motion, and the orbital elements. Figure 1 shows the magnitude distribution of all detection from the year 2005. The solid line indicates the system sensitivity (scale at right-hand side) as determined from independent calibration measurements. All magnitudes have been reduced from apparent magnitudes to so-called absolute magnitudes by correcting for the illumination phase angle. For the scattering properties we assumed a simple Lambertian sphere. No reduction to a common distance has been done because of the uncertainties of the determined orbits. The indicated object sizes were derived by assuming a Bond albedo of 0.1. The bimodal distribution with a large population of faint, uncorrelated objects is seen throughout all ESA surveys since 1999 (see [1], [2]).

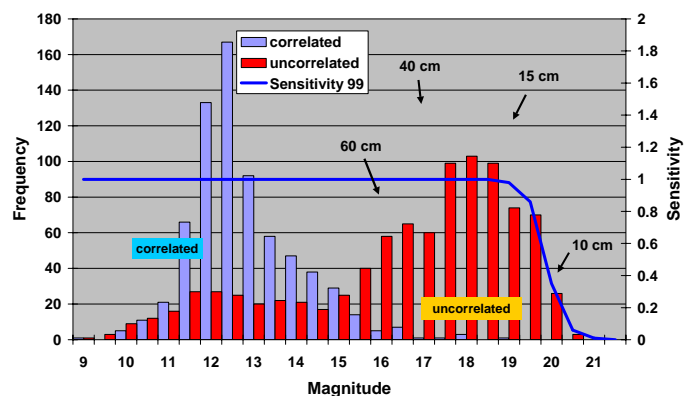


Figure 1: Magnitude distribution for the detections from January 2005 to December 2005 (magnitudes corrected for phase angle). The solid line indicates the system sensitivity (scale at right-hand side) as determined from independent calibration measurements.

A very important characteristic of the debris population is the distribution of the orbital planes of the debris objects.

	Aug/Sept 1999 GEO	Jan – Jul 2001 GEO	Jan – Dec 2002 GEO/GTO	Jan – Dec 2003 GEO/GTO	Jan – Dec 2004 GEO/GTO	Jan – Dec 2005 GEO/GTO
Frames	5'400	65'000	81'800	66'000	49'500	59'500
Scanned Area	895 deg ²	11'200 deg ²	13'700 deg ²	10'600 deg ²	7'800 deg ²	8'800 deg ²
Total Observing Time	13 nights (49 h)	82 nights (548 h)	96 nights (691 h)	88 nights (559 h)	70 nights (417 h)	85 nights (495 h)
GTO / Follow-up	– / –	– / 18 h	200 h / 71 h	245 h / 103 h	145 h / 93 h	205 h / 141 h
Correlated detec- tions	180	2'023	1960	1258	483	708
Correlated ob- jects	56	448	849	862	303	443
Uncorrelated detections	348	1'587	2'389	1812	711	922

Table 1: ESA GEO/GTO survey campaigns.

Figure 2 and Figure 3 show this distribution, in terms of inclination i as a function of the right ascension of the ascending node Ω , for all correlated and uncorrelated detections of the year 2005. The distinct curve followed by the correlated objects is caused by the well-known 53-year precession period of the orbital planes of uncontrolled objects in GEO. Assuming that the objects started with orbits of $i = 0^\circ$, the current position in the diagram stands for the time since the end of active inclination control. The orbits gradually evolve along the feature seen in Figure 2. More precisely they evolve from a point at about ($\Omega \approx 100^\circ$, $i \approx 0^\circ$) to higher inclinations and smaller right ascension of the node until they reach the maximum inclination of $i = 15^\circ$ after 26.5 years. This evolutionary pattern is also present in the distribution of the uncorrelated detections. In addition, however, there is a significant ‘background’ component with a homogeneous distribution in the (Ω, i)-space, as well as distinct clusters of detections.

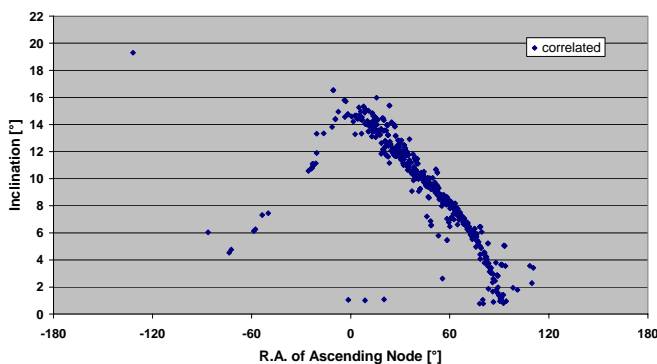


Figure 2 Inclination versus right ascension of ascending node for the correlated detections from January 2005 to December 2005.

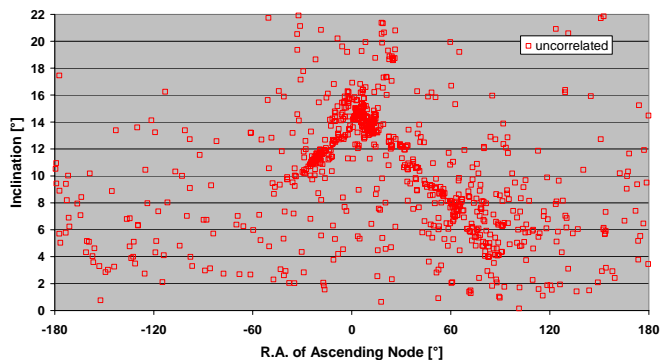


Figure 3: Inclination versus right ascension of ascending node for the uncorrelated detections from January 2005 to December 2005.

The most prominent concentrations in Figure 3 are found at ($\Omega \approx 20^\circ$, $i \approx 11^\circ$), ($\Omega \approx 5^\circ$, $i \approx 14.5^\circ$), ($\Omega \approx 10^\circ$, $i \approx 13.5^\circ$), and at ($\Omega \approx 65^\circ$, $i \approx 7.5^\circ$).

Both figures show no objects at $i = 0^\circ$ inclination because this region was not included in the survey.

There are two important issues to note: a) the ‘detections’ of one year may contain multiple observations of objects, and b) the orbital elements plotted in Figure 2 and Figure 3 were derived assuming circular orbits.

For the ESA Tenerife surveys we expect to see each object on average five times within one year [3]. However, the surveys are quite homogeneous in term of the probability to see objects in specific orbital planes, which means that structures in the (Ω, i)-space cannot be explained by multiple sightings of objects.

The circular orbit hypothesis, on the other hand, is more critical. For a certain fraction of the detections this will lead to significantly wrong orbital elements. This ‘contamination’ by in fact elliptical orbits may be substantial. In a GEO survey objects with high eccentricities are preferentially detected when they are near the apogee. By inferring circular orbits for these objects we interpret the change in the true anomaly near the apogee as the mean motion of a circular orbit. The velocity of an object in an elliptical orbit at the apogee is slower than the corresponding velocity of an object on a circular orbit with a radius equal to the apogee radius of the former. This in turn means that the radius of the inferred circular orbit exceeds the apogee radius of the elliptical orbit [4]. Indeed, in the detections from 2005 we find 360 out of 922, which have radii larger than 44’164 km – 2’000 km more than the nominal GEO radius.

Figure 4 shows the (Ω, i) -diagram for the subset of the 2005 detections with radii smaller than 44’164 km and Figure 5 with radii larger than 44’164 km, respectively. Restricting the data set to small radii does reduce the ‘background’ component (Figure 4), although not completely. The distribution of the orbital planes of the detections with large radii – presumably object on elliptical orbits – still shows some structure, and a general concentration along the ‘evolution path’ but with a much larger spread (Figure 5). We conclude a) that part of the ‘homogeneous background’ may be due to ‘contamination’ by elliptical orbits, and b) that some of the detections in the clusters show strong evidence to be objects on elliptical orbits.

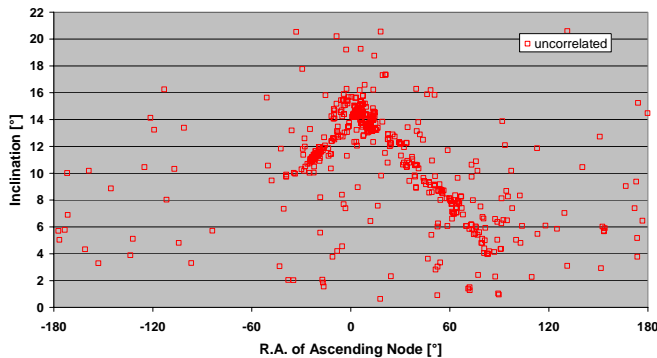


Figure 4: Inclination versus right ascension of ascending node for a subset of the uncorrelated detections from January 2005 to December 2005. Only detections with an inferred radius of the circular orbit smaller than 44’164 km are plotted.

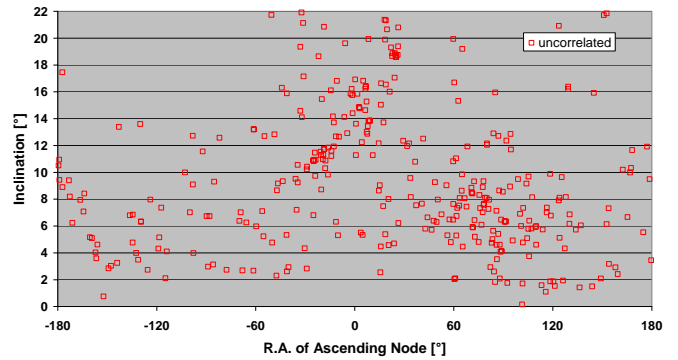


Figure 5: Inclination versus right ascension of ascending node for a subset of the uncorrelated detections from January 2005 to December 2005. Only detections with an inferred radius of the circular orbit larger than 44’164 km are plotted.

EVOLUTION OF THE DEBRIS CLUSTERS – COMPARISON WITH SIMULATIONS

In order to learn more about the nature of the clusters and to eventually trace them back to some parent objects we may study the evolution of the clusters with time. The ESA surveys provide a unique data set for this purpose. The observations are rather homogeneous and cover a time interval of currently more than 6 years. Figure 6 shows the (Ω, i) -diagrams for the uncorrelated detections for the years 2001 through 2005. A careful inspection reveals at least 8 distinct clusters in the 2001 and 2002 data. The motion of the individual clusters along the evolution path may be clearly identified, at least for the most massive clusters. In order to understand this observed behavior more quantitatively we simulated the evolution of four observed clusters and compared the results with the observations.

The input data for the simulation was derived from the 2002 data set where four clusters were defined by manually selecting the members in the (Ω, i) -diagram (Figure 7). We furthermore restricted the clusters to members with radii (at the observation epoch) between 40’164 km and 44’164 km.

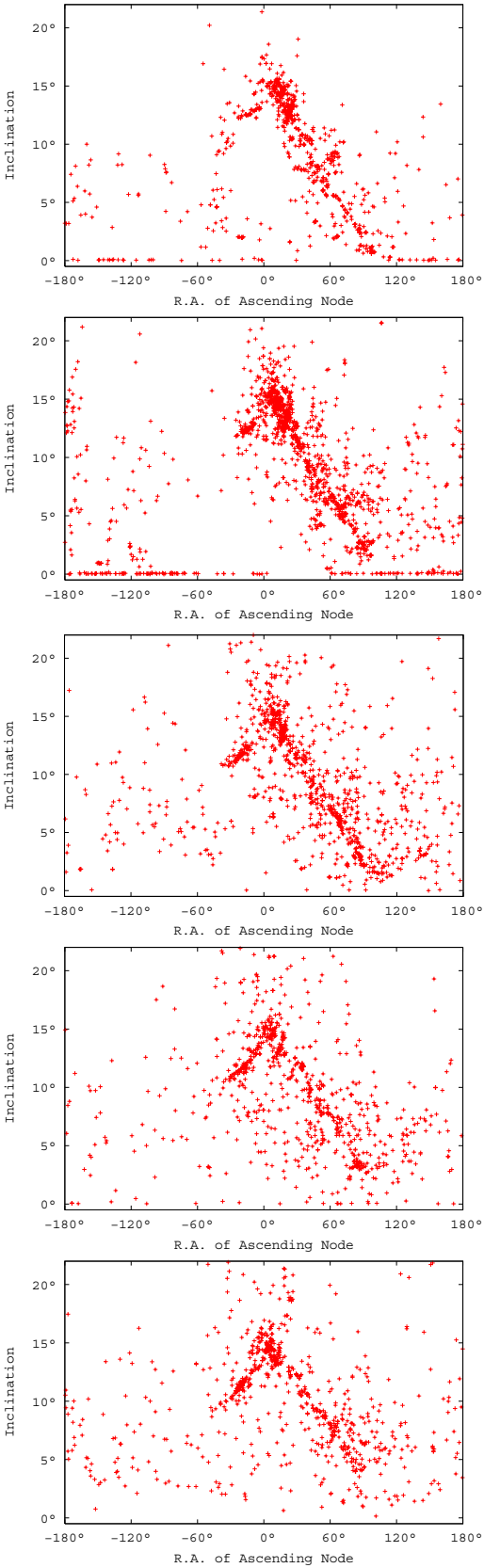


Figure 6: (Ω, i) -diagrams of the uncorrelated detections of the years 2001 through 2005 from top to bottom.

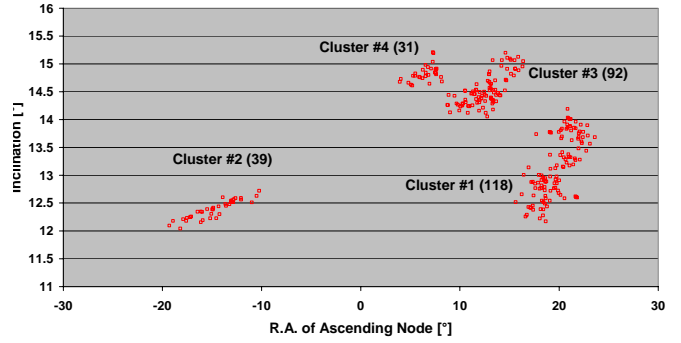


Figure 7: (Ω, i) -diagrams of the four manually defined clusters from the 2002 data. Numbers in parentheses indicate the numbers of objects forming the cluster.

The clusters were then propagated over 48 years using the numerical integrator SATORB described in [5], [6]. The force model included Earth's potential coefficients up to terms of degree and order 12, the gravitational attraction of the Sun and the Moon (JPL DE200 ephemerides), and a direct radiation pressure parameter, which can be related to an area-to-mass ratio of the objects. The modeling of the direct radiation pressure is including eclipses due to the Earth's shadow. In a first simulation we assumed the canonical value of $0.02 \text{ m}^2\text{kg}^{-1}$ for the area-to-mass ratio of all objects. Figure 8 shows the location of cluster #3 in the (Ω, i) -diagram over the next 48 years. The corresponding (Ω, i) -diagram in polar coordinates is given in Figure 9. The figures primarily show the well-known precession motion with a period of 53 years. The orbital planes of the individual cluster members are precessing with very similar rates and the cluster thus remains rather compact in the (Ω, i) -space (Figure 9).

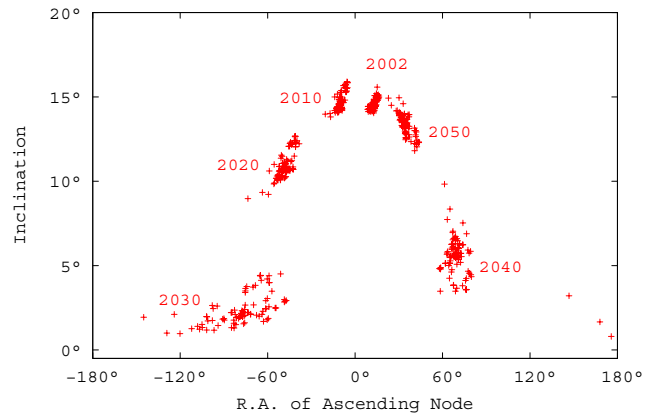


Figure 8: Propagation of cluster #3 over 48 years assuming an area-to-mass ratio of $0.02 \text{ m}^2\text{kg}^{-1}$.

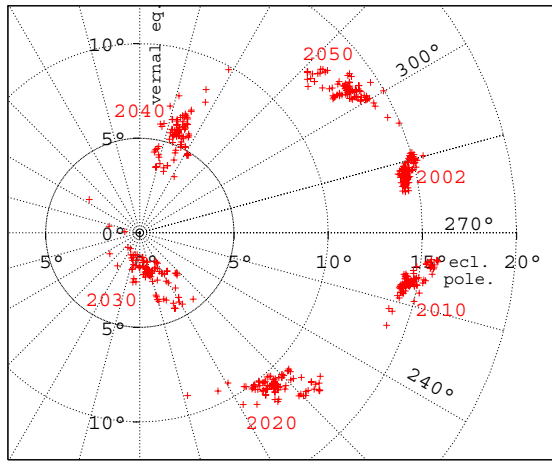


Figure 9: Propagation of cluster #3 over 48 years assuming an area-to-mass ratio of $0.02 \text{ m}^2\text{kg}^{-1}$. Polar plot of inclination and right ascension of ascending node.

The ESA surveys for objects in highly elliptical orbits, however, have revealed a population of objects with extremely high area-to-mass ratios of up to $30 \text{ m}^2\text{kg}^{-1}$ [7], [4]. It is therefore rather likely that the clusters consist of objects with a mixture of very different area-to-mass ratios. The evolution of the orbits of objects with area-to-mass ratios larger than $1 \text{ m}^2\text{kg}^{-1}$ significantly differs from the evolution of objects with area-to-mass ratios of the order of a few $0.1 \text{ m}^2\text{kg}^{-1}$ or less. The solar radiation pressure is perturbing the orbits of these objects considerably. The main effects are short-periodic variations of the eccentricity and of the inclination with periods of about one year (actually one nodal year; see Figure 10). Long-periodic variations are also observed, especially for very high area-to-mass ratios. (Note that radiation pressure is a conservative force and that therefore the semimajor axis is not changed significantly.) As a consequence the precession motion of the orbital planes is different with respect to GEO objects in near-circular orbits. An increased area-to-mass ratio results in a shorter precession period and an increased mean inclination. Figure 11 and Figure 12 illustrate the evolution of the orbital planes of cluster #4 over a time interval of 28 years assuming an area-to-mass ratio of $15 \text{ m}^2\text{kg}^{-1}$. (Cluster #3 would behave very similar, but cluster #4 was chosen because it has less objects.) Note the much shorter precession period of the order of 30 years and the differences in the inclination range when compared with Figure 8 and Figure 9.

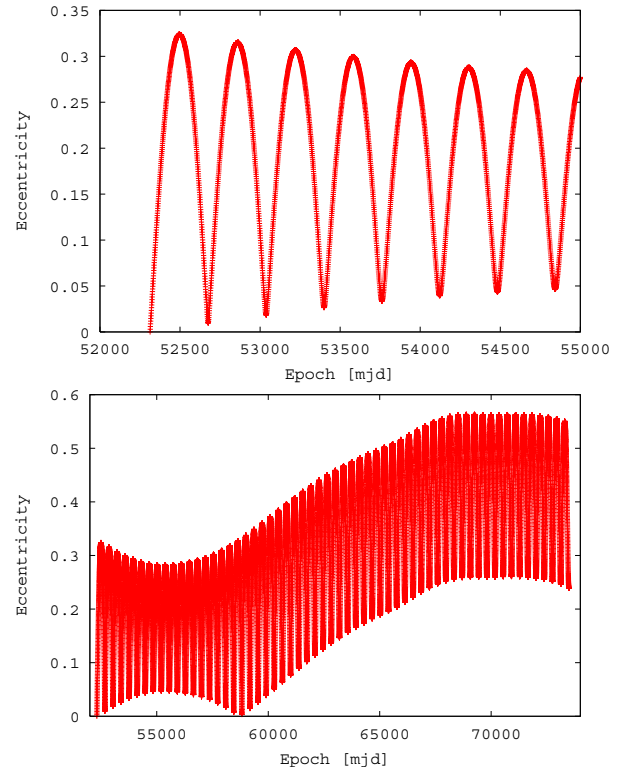


Figure 10: Short-periodic (top) and long-periodic (bottom) variations of the eccentricity for an object with an area-to-mass ratio of $15 \text{ m}^2\text{kg}^{-1}$. (The object was arbitrarily chosen from cluster #4.)

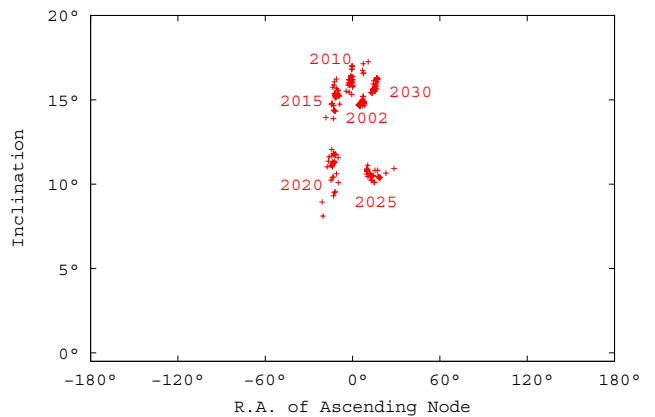


Figure 11: Propagation of cluster #4 over 28 years assuming an area-to-mass ratio of $15 \text{ m}^2\text{kg}^{-1}$.

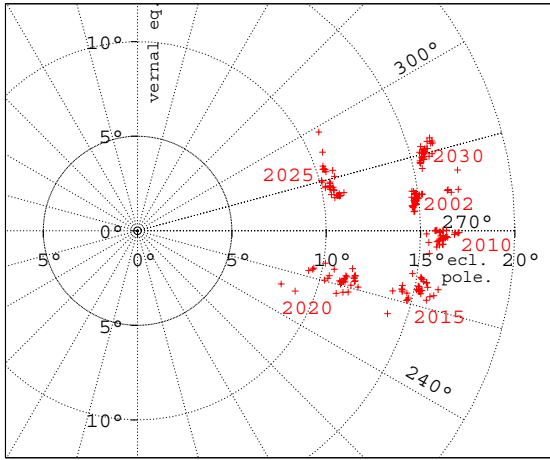


Figure 12: Propagation of cluster #4 over 28 years assuming an area-to-mass ratio of $15 \text{ m}^2\text{kg}^{-1}$. Polar plot of inclination and right ascension of ascending node.

Clusters seen in the data from a single year could be artifacts produced by observational biases. One indication that they are real is the fact that some of them appear in the ESA surveys for over more than 6 years. We could construct even more convincing evidence for the realness of the clusters by showing that the observed clusters dynamically evolve as expected. Moreover a comparison of the observed evolution with simulations may give some indications on the area-to-mass ratios of the objects in the clusters.

In Figure 13 to Figure 15 we compare the observed orbital planes from the years 2003 to 2005 with the four propagated clusters observed in the year 2002. The clusters were propagated to the middle of each year using an area-to-mass ratio of $0.02 \text{ m}^2\text{kg}^{-1}$. We note that observed evolution of the clusters #1, #2, and #3 qualitatively matches with the corresponding propagated clusters of the year 2002. This simply proves that at least clusters #1 to #3 are real. Cluster #4 seems to dissolve over time and its position in Figure 15 is offset from the prediction.

Changes in the positions of the propagated clusters are not easily seen when comparing the figures. However, direct comparisons of the observations of one year with clusters propagated for a different year would show obvious mismatches. It is in any case not possible to compare the details because we did most likely not observe the same members of the clusters throughout the years and furthermore the observations correspond to different epochs within a particular year (i.e. they have not been propagated to e.g. the middle of the year). Moreover

the simulations do not account for the likely possibility that the real clusters contain objects with a wide range of different area-to-mass ratios. Such clusters would dissolve over time due to the different precession rates of the orbital planes. Cluster #4 could be an example of this type. High area-to-mass ratio objects could thus be responsible for a part of the ‘homogeneous background’ seen in the (Ω, i) -diagrams.

That fact that the clusters #1 to #3 stay compact in the (Ω, i) -space over four years is also restricting the range of area-to-mass ratios for the cluster members. Only a small number of objects in these clusters can have extreme area-to-mass ratios significantly larger than $10 \text{ m}^2\text{kg}^{-1}$. Long-term monitoring of the clouds is important to better understand this issue, which in turn is crucial to identify the physical properties of the objects and finally the potential progenitors.

Eventually measurements of the area-to-mass-ratio of a statistically significant number of individual cluster members are required. This is only possible through monitoring the dynamical evolution of individual objects of the clusters. Technically this means that follow-up observations (likely involving multiple sites) of a subset of the objects must be performed in order to obtain sufficiently long arcs of observations to derive the area-to-mass ratios from the orbit modeling.

These efforts will yield the necessary input data to improve the ESA MASTER debris population model for high-altitude regions. MASTER, as well as the debris models of other space agencies, currently does not consider debris with very high area-to-mass ratios.

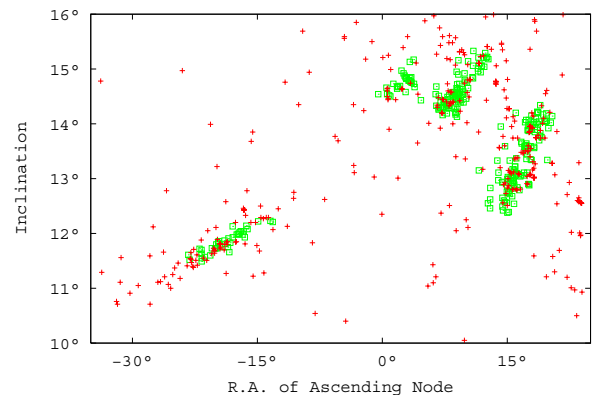


Figure 13: Comparison of the observed orbital planes from 2003 (crosses) with the four propagated clusters observed in the year 2002 (squares; area-to-mass ratio of $0.02 \text{ m}^2\text{kg}^{-1}$).

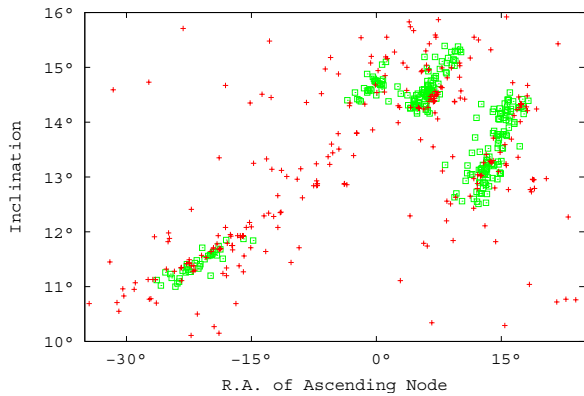


Figure 14: Comparison of the observed orbital planes from 2004 (crosses) with the four propagated clusters observed in the year 2002 (squares; area-to-mass ratio of $0.02 \text{ m}^2\text{kg}^{-1}$).

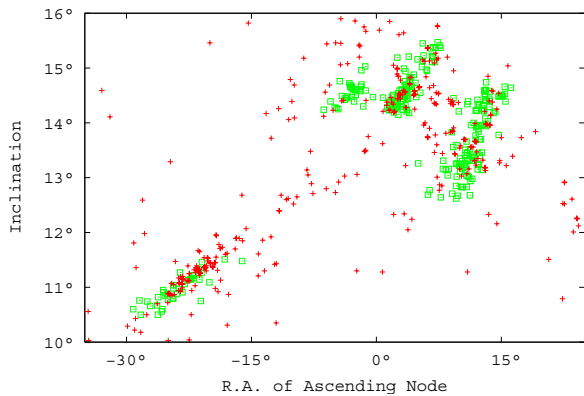


Figure 15: Comparison of the observed orbital planes from 2005 (crosses) with the four propagated clusters observed in the year 2002 (squares; area-to-mass ratio of $0.02 \text{ m}^2\text{kg}^{-1}$).

CONCLUSION

ESA has established a long-term survey program to study the space debris environment at high altitudes. Since 2001 the ESA 1-meter telescope in Tenerife, Canary Islands, is used during about 120 to 140 nights per year to search and follow-up space debris in GEO, GTO and other high-altitude orbits. These surveys discovered a substantial population of debris objects with sizes between one meter and 10 centimeters located in these regions. This population shows distinct clusters in the orbital element space (orientation of the orbital planes). Follow-up observations allowed determining 6-parameter orbits for a subset of the detections and eventually led to the discovery of a population of objects with extremely high area-to-mass ratio objects.

The ESA observations are rather homogeneous and cover a time interval of currently more than 6 years. The data set thus provides a unique possibility to study the evolution of the debris environment. By monitoring in particular the evolution of the clusters we may learn more about the nature of the clusters. The data set has been and will be used as indispensable input for the ESA MASTER debris population model.

In order to exclude the possibility that the clusters are observational artifacts we compared the observed dynamical evolution of the clusters with simulations. For the latter we identified a series of four clusters in the 2002 data set and propagated them forward in time by numerically integrating the orbits of their members. The comparison proved that the clusters are real. We also showed that clusters dissolve within a few years if their members have a wide range of area-to-mass ratios. As a consequence we expect that part of the ‘homogeneous background’ seen in the (Ω, i) -diagrams may be due to high area-to-mass ratio objects.

The distribution of the area-to-mass ratios in the clusters is currently unknown. Further monitoring is required to provide constraints for the area-to-mass ratios of the cluster members by analyzing the long-term evolution of the clusters. Such monitoring will eventually enable the identification of the parent objects of the clusters.

REFERENCES

- [1] Schildknecht, T., R. Musci, M. Ploner, S. Preisig, J. de Leon Cruz, and H. Krag, Optical Observation of Space Debris in the Geostationary Ring, 3rd European Conference on Space Debris, 19 – 21 March 2001, ESOC, Darmstadt, Germany, 2001.
- [2] Schildknecht, T., R. Musci, M. Ploner, G. Beutler, W. Flury, J. Kuusela, J. de Leon Cruz, and L. de Fatima Dominguez Palmero, Optical Observations of Space Debris in GEO and in Highly-eccentric Orbits, 34th COSPAR Scientific Assembly, Oct 10 - 19, 2002, Houston, Texas, USA, Advances in Space Research, Vol. 34, pp. 901–911, 2004.
- [3] Jehn, R., S. Ariafar, T. Schildknecht, R. Musci, and M. Oswald, Estimating the Number of Debris in the Geostationary Ring, Acta Astronautica, Vol. 59, No. 1-5, pp. 84-90, 2006.
- [4] Schildknecht, T., Optical Surveys for Space Debris, Astronomy and Astrophysics Review, in Press.
- [5] G. Beutler, Methods of Celestial Mechanics, 2 Volumes, Springer, 2005.
- [6] G. Beutler, T. Schildknecht, U. Hugentobler, W. Gurtner, Orbit determination in satellite geodesy, Adv. Space Res., 31, 1853-1868, 2003.
- [7] Schildknecht, T., R. Musci, W. Flury, J. Kuusela, J. de Leon, and L. de Fatima Dominguez Palmero, Optical Observations of Space Debris in High-Altitude Orbits, 4th European Conference on Space Debris, April 18-20, ESOC, Darmstadt, Germany, ESA Publication SP-587, pp. 113–118, 2005.